

# Numerical estimates of the accretion rate on to intermediate-mass black holes

C. Pepe<sup>1,2★</sup> and L. J. Pellizza<sup>1,2</sup>

<sup>1</sup>*Instituto de Astronomía y Física del Espacio, Casilla de Correos 67, Suc. 28, 1428 Buenos Aires, Argentina*

<sup>2</sup>*Consejo Nacional de Investigaciones Científicas y Técnicas, CONICET, Argentina*

Accepted 2013 January 11. Received 2013 January 11; in original form 2012 November 21

## ABSTRACT

The existence of intermediate-mass ( $\sim 10^3 M_{\odot}$ ) black holes (IMBHs) in the centre of globular clusters has been suggested by different observations. The X-ray sources observed in NGC 6388 and in G1 in M31 could be interpreted as being powered by the accretion of matter on to such objects. In this work, we explore a scenario in which the black hole accretes from the cluster interstellar medium, which is generated by the mass-loss of the red giants in the cluster. We estimate the accretion rate on to the black hole and compare it to the values obtained via the traditional Bondi–Hoyle model. Our results show that the accretion rate is no longer solely defined by the black hole mass and the ambient parameters but also by the host cluster itself. Furthermore, we find that the more massive globular clusters with large stellar velocity dispersion are the best candidates in which accretion on to IMBHs could be detected.

**Key words:** accretion, accretion discs – black hole physics – globular clusters: general.

## 1 INTRODUCTION

The existence of intermediate-mass black holes ( $10^2$ – $10^4 M_{\odot}$ , IMBHs) was suggested, among other observations, by the detection of ultraluminous X-ray sources (ULXs) in nearby galaxies (see Feng & Soria 2011 for a review). The X-ray fluxes and the distances measured for these sources imply luminosities (assuming isotropic emission)  $L > 10^{39} \text{ erg s}^{-1}$ , in excess of the Eddington luminosity for an accreting stellar-mass compact object ( $M \sim 10 M_{\odot}$ ). The simplest explanation for these high luminosities is the presence of accreting objects with masses in the range of those of IMBHs, but other hypotheses have been proposed. K rding, Falcke & Markoff (2002) suggested that the emission of ULXs could be beamed, hence implying lower luminosities for these sources, while King et al. (2001) proposed that ULXs emit indeed in a super-Eddington regime with mild geometrical collimation of their photon emission (a factor of  $\lesssim 10$ ) due to outflows. Although in these alternative models accreting stellar-mass black holes could explain the observed luminosities, they fail to account for sources with  $L \gtrsim 10^{41} \text{ erg s}^{-1}$ , which still require the accreting compact object to be an IMBH (Feng & Soria 2011).

On the other hand, different theoretical models for the origin of IMBHs have been proposed. According to Fryer & Kalogera (2001), IMBHs would be the dead fossils of primordial (Population III) stars, while Miller & Hamilton (2002) have shown that black holes of  $10^3 M_{\odot}$  could form in globular clusters (GCs) as a consequence

of the merger of stellar-mass black holes. A similar mechanism was proposed by Portegies Zwart et al. (2004), who have shown that a runaway collision of massive stars in a GC results in an IMBH at its centre. Hence, GCs have become the main candidates to host these objects. The extrapolation of the relation between the central black hole mass and the bulge mass of galaxies (e.g. Magorrian et al. 1998) also points to the existence of IMBHs in GCs.

Following the predictions of theoretical models, several attempts to detect IMBHs at the centres of GCs were done. Stellar density profiles and stellar dynamics measurements in the central regions of some GCs suggest the existence of central objects with masses  $\sim 10^3 M_{\odot}$ . Miocchi (2007) developed a model for the stellar distribution in GCs, including the effects of an IMBH. Those models containing an IMBH yield results consistent with the surface brightness and velocity dispersion profiles obtained by Noyola & Gebhardt (2006) for the Galactic GCs NGC 2808, NGC 6388, M80, M13, M62 and M54, and also G1 in M31. Van den Bosch et al. (2006) constructed dynamical models of M15 and estimated the central mass to be  $3400 M_{\odot}$ . However, the nature of this concentrated mass cannot be distinguished: it could be either an IMBH or a large number of stellar-mass compact objects, or a combination of both. On the other hand, McLaughlin et al. (2006) fitted the proper motion dispersion profile of 47 Tuc, obtaining an estimate of its central point mass of  $1000$ – $1500 M_{\odot}$  at the 68 per cent confidence level. Noyola et al. (2010) analysed the surface brightness and velocity dispersion profiles of  $\omega$  Cen. Both profiles show a central cusp, a  $4000 M_{\odot}$  IMBH being the best explanation for these observations. Gebhardt, Rich & Ho (2002) reported a  $2 \times 10^4 M_{\odot}$  point mass at the centre of G1, based on photometric and

★E-mail: carolinap@iafe.uba.ar

kinematical data in the central areas. However, other authors arrived at different conclusions. For example, van der Marel & Anderson (2010) and Baumgardt et al. (2003) constructed dynamical models for  $\omega$  Cen and G1, respectively, claiming that the presence of an IMBH is not needed to fit the available data. Because of this lack of consensus, the study of IMBHs is still an open issue and efforts need to be made in order to clarify the subject. Moreover, although kinematical and photometric data are suitable to show the presence of central mass concentrations in GCs, at present they are unable to determine the nature of these concentrations, namely if they comprise a single massive object or a collection of stellar-mass remnants. Complementary data are needed to prove any of these hypotheses.

As in other systems containing compact objects, the detection of ongoing accretion may help to place constraints on the existence and properties of IMBHs. Hence, searches of central X-ray sources have been performed in several GCs. The detection of central sources with properties consistent with those expected from an IMBH has been reported only for two clusters: NGC 6388 and G1 (Nucita et al. 2008; Kong et al. 2010). In other clusters, only upper limits for the X-ray luminosity of a central source have been obtained, constraining it to be lower than  $\sim 10^{31} - 10^{32}$  erg s<sup>-1</sup> (MacCarone 2004, and references therein). Assuming that the IMBH accretes from the intracluster medium (ICM), that the ICM has a density similar to that measured by Freire, Kramer & Lyne (2001) in NGC 104 and that the radiative efficiency is similar to that observed in other black hole systems, MacCarone (2004) concludes that the accretion rate must be far lower than that predicted by the standard Bondi–Hoyle model (Bondi & Hoyle 1944) in order to match the non-detections of central sources. Based on the correlation between X-ray and radio luminosity of accreting stellar-mass black holes (Gallo, Fender & Pooley 2003), this author also argues that the radio emission of the system would be more easily detectable than the X-ray emission. However, no central radio source has been detected in Galactic GCs which, according to MacCarone (2004), imposes strong constraints on the masses of the hypothetical IMBHs. Only Ulvestad, Greene & Ho (2007) reported the detection of a radio source at about 1 arcsec from the centre of G1 in M31. They concluded that this radio emission is consistent with that expected for a  $2 \times 10^4 M_{\odot}$  IMBH accreting at the centre of the cluster. Nevertheless, this result has been challenged by recent observations (Miller-Jones et al. 2012).

It is clear that the detection of (or the failure to detect) accretion-powered sources in the centres of GCs is crucial for the investigation of the existence and nature of IMBHs. In this context, the interpretation of both X-ray and radio data has been done in the past using simple models. In particular, Bondi–Hoyle accretion has been used, which assumes a point mass (the IMBH) accreting from a homogeneous, static medium. In a previous work (Pepe, Pellizza & Romero 2012), we studied the accretion of dark matter on to IMBHs. We took into account the gravitational pull of the cluster on the accreted matter and found that the accretion rate depends on the cluster mass, unlike the Bondi–Hoyle accretion rate that scales as the square of the IMBH mass. The Bondi–Hoyle accretion rate is retrieved only for ultrarelativistic fluids, which are not influenced by the presence of the cluster. As the ICM is a non-relativistic fluid, we expect that its behaviour departs from that predicted by the standard Bondi–Hoyle theory. Moreover, the ICM of a GC is not a homogeneous, static medium, because it is fed by the red giant stars and cleansed by the passages of the cluster through the Galactic plane (Roberts 1988). The influence of these effects on the accretion rate should be quantified to make a proper comparison between models and X-ray or radio observations.

In this work, we develop a simple numerical model for the accretion flow of the ICM on to an IMBH at the centre of a GC, including the cluster gravitational pull and the ICM sources. We estimate the accretion rate and its dependence on both the IMBH mass, and the GC and ICM properties, and compare them with those predicted by the standard Bondi–Hoyle model. In Section 2, we describe the hydrodynamical equations of the flow and discuss its main characteristics, while in Section 3 we solve these equations for Milky Way GCs with different masses of the IMBHs and temperatures of the ICM, stressing the differences between our results and those obtained with the Bondi–Hoyle model. Finally, in Section 4 we discuss the consequences of our results on the search for IMBHs, and present our conclusions.

## 2 THE MODEL

### 2.1 Hydrodynamical equations

In order to understand the accretion process by an IMBH in a GC, we study the dynamics of the ICM in the presence of the cluster plus IMBH gravitational potential. We aim at computing the accretion rate, to compare it with the standard Bondi–Hoyle theory. The ICM is generated by the mass-loss of the red giants of the cluster. Assuming that the distribution of these stars follows the stellar mass density of the cluster, and that the average mass-loss rate is the same for all red giants, the rate at which the density of the ICM increases due to the injection of matter by these stars at any position within the cluster can be written as

$$\dot{\rho} = \alpha \rho^*, \quad (1)$$

where  $\rho^*$  is the stellar mass density. The right-hand side describes the gas injection by the stars at a fractional rate  $\alpha$ , for which theoretical and observational works obtain estimations in the range  $10^{-14} - 10^{-11}$  yr<sup>-1</sup> (Fusi Pecci & Renzini 1975; Scott & Rose 1975; Dupree et al. 1994; Mauas, Cacciari & Pasquini 2006, and references therein). The cluster plus IMBH gravitational field can be described by the model developed by Mocchi (2007). This model is basically a King (1966) model with the presence of a black hole at the centre of the cluster, which modifies the dynamics of the stars in the inner region. Following Scott & Rose (1975), we assume that the ICM is an ideal gas, and that its flow can be considered steady, spherically symmetric and isothermal. Under these hypotheses, the flow is governed by continuity and Euler’s equations. The former is

$$\frac{1}{r^2} \frac{d}{dr} (\rho r^2 u) = \alpha \rho^*, \quad (2)$$

where  $r$  is the radial coordinate, and  $u$  and  $\rho$  are the velocity and density of the flow, respectively. Euler’s equation is

$$\rho u \frac{du}{dr} = -\frac{k_B T}{\mu} \frac{d\rho}{dr} - \frac{GM(r)\rho}{r^2} - \alpha u \rho^*, \quad (3)$$

where  $G$  is the gravitational constant,  $k_B$  is Boltzmann’s constant,  $\mu$  is the mean molecular mass of the ICM, and  $M(r)$  is the sum of the stellar mass  $M^*(r)$  inside radius  $r$  and the central IMBH mass  $M_{\text{BH}}$ . It is assumed here that the material is injected with null velocity in the flow.

These equations can be simplified introducing the variable  $\tilde{q} = q/\alpha$ , where  $q = \rho u r^2$  is the bulk flow, giving

$$\frac{d\tilde{q}}{dr} = \rho^* r^2, \quad (4)$$

$$\frac{du}{dr} = \frac{u}{u^2 - c_s^2} \left( \frac{2c_s^2}{r} - \frac{GM(r)}{r^2} - \frac{(u^2 + c_s^2)r^2 \rho^*}{\tilde{q}} \right), \quad (5)$$

where  $c_s = k_B T \mu^{-1}$  is the sound speed. It is important to note that, with this definition, we can solve the equations independently of  $\alpha$ . However,  $\alpha$  must be known to calculate the density and the accretion rate.

Equation (4) can be integrated, giving

$$\tilde{q} = \int_0^r \rho^* r'^2 dr' + \tilde{q}_0 = \frac{M^*(r)}{4\pi} + \tilde{q}_0, \quad (6)$$

where the integration constant  $\tilde{q}_0$  is proportional to the accretion rate of the black hole. Although the integration should be done from the Schwarzschild radius, this radius is negligible with respect to all the scales in our model; hence, we take it as zero.

To perform the integration, we define adimensional variables  $\xi = r r_0^{-1}$ ,  $\psi = u \sigma^{-1}$  (and, therefore,  $\psi_s = u_s \sigma^{-1}$ ),  $\omega = \tilde{q} (\rho_0 r_0^3)^{-1}$ ,  $\Omega^*(\xi) = M^*(r) (4\pi \rho_0 r_0^3)^{-1}$ ,  $\Omega_{\text{BH}} = M_{\text{BH}} (4\pi \rho_0 r_0^3)^{-1}$  and  $\Omega(\xi) = \Omega^*(\xi) + \Omega_{\text{BH}}$ , where  $r_0$  is the King radius,  $\rho_0$  is the cluster central density and  $\sigma^2 = 4\pi G \rho_0 r_0^2 / 9$  is the velocity dispersion parameter. With these definitions, equations (5) and (6) can be rewritten as

$$\omega = \Omega^*(\xi) + \omega_0, \quad (7)$$

$$\frac{d\psi}{d\xi} = \frac{\psi}{\psi^2 - \psi_s^2} \left( \frac{2\psi_s^2}{\xi} - \frac{d\omega(\psi_s^2 + \psi^2)}{d\xi} - \frac{9\Omega(\xi)}{\xi^2} \right). \quad (8)$$

These equations describe the flow dynamics in our model. They represent an extension of the Bondi–Hoyle expressions to the case in which the fluid has sources, and a gravitational field other than that of the accretor acts on it. These effects are represented by the second and the third terms in parentheses on the right-hand side of equation (8), and the first term on the right-hand side of equation (7). The boundary conditions and integration method for this set of equations are described in the following section.

## 2.2 Boundary conditions

In order to integrate equation (8), boundary conditions must be set. Far away from the accreting black hole, the velocity of the flow must be positive as there is no matter source outside the cluster. On the other hand, on the black hole surface, matter can only fall inwards as there is no pressure gradient that supports the gravitational pull of the black hole and the cluster. As a direct consequence, there exists a stagnation radius  $\xi_{\text{st}}$  at which  $u = 0$ . Evaluating equation (7) at the stagnation radius gives

$$\Omega^*(\xi_{\text{st}}) = -\omega_0, \quad (9)$$

which means that all the matter ejected by the red giants inside  $\xi_{\text{st}}$  is accreted by the IMBH. This is a direct consequence of the hypothesis of stationarity. Thus, the stagnation radius separates two distinct regions in space: a regime of accretion develops in the inner region and a wind solution exists in the outer one. It is important to highlight that, so far, the stagnation radius cannot be uniquely defined by these equations. For every stagnation radius there exists a solution to the equations. However, they are not all physically acceptable, as the Rankine–Hugoniot conditions for the continuity of the flow at the stagnation radius require that densities at both sides of  $\xi_{\text{st}}$  must be equal.

As in the Bondi–Hoyle problem (e.g. Frank, King & Raine 2002), it can be seen from equation (8) that there exist singular values  $\xi_s$  (called sonic radii) for which either the velocity equals the sound

speed in the medium or the acceleration of the flow is null. This is the case when the expression in parentheses in equation (8) cancels,

$$2\psi_s^2 \left( \frac{1}{\xi} - \frac{1}{\omega} \frac{d\omega}{d\xi} \right) - \frac{9\Omega(\xi)}{\xi^2} = 0. \quad (10)$$

For the same reasons of the classical analysis of the Bondi–Hoyle problem, only the transonic curves are consistent with the properties of an accretion flow.

Given that  $\xi_{\text{st}}$  is not known a priori, the problem was solved numerically for a grid of values of  $\xi_{\text{st}}$  between 0 and the cluster tidal radius. For each one of these values, sonic radii in the inner and outer regions were searched for, using a bisection scheme to find the roots of equation (10). Then, equation (8) was integrated (via a fourth-order Runge–Kutta scheme) inwards from the outer sonic point and outwards from the inner one, up to the stagnation radius. The difference between the densities at each side of the stagnation point was calculated for each  $\xi_{\text{st}}$ , and interpolated to zero to find the true stagnation radius. Once this value was found, we integrated equations (7) and (8) to obtain the true density and velocity profiles.

## 3 RESULTS

### 3.1 Individual clusters

We first explore the behaviour of the accretion flow in a given GC. The cluster is represented by the value of the concentration  $c_{\text{GC}}$  (defined as the ratio of the cluster tidal radius to  $r_0$ ), and two of the three parameters  $r_0$ ,  $\rho_0$ ,  $\sigma$ . These parameters together with the IMBH mass allow us to construct the Miocchi (2007) model for the stellar mass  $M(r)$  of the cluster uniquely. The concentration and IMBH mass define the shape of  $M(r)$ , while the other parameters merely set its physical scale. Note that the same is true for our hydrodynamical model, as the flow can be fully expressed using non-dimensional variables defined in terms of those scaling parameters. Thus, for a given GC there are only two free parameters in our model: the non-dimensional temperature (or the sound speed  $c_s/\sigma$ ) and IMBH mass  $\Omega_{\text{BH}}$ .

With the above considerations in mind, we took four sample GCs: NGC 7078 (M15), Liller 1, NGC 6626 (M28) and NGC 5139 ( $\omega$  Cen), which span the concentration range of Milky Way GCs (see Table 1), and for each one we constructed different flow models, performing a scan of the two free parameters. Although NGC 7078 and Liller 1 have almost the same value for the concentration, they differ in the scaling parameters, which allows us to extend the range of the non-dimensional free parameters. The temperature covers the range 5000–15 000 K, which is the range expected for the ICM (Scott & Rose 1975; Knapp et al. 1996; Priestley, Ruffert & Salaris 2011). The IMBH mass ranges from  $10^2$  up to  $10^4 M_\odot$ . Heavier masses would produce a strong effect on the stellar dynamics and structure of the cluster, which is not observed, while for lower

**Table 1.** GC parameters taken from Harris (1996). The central density was estimated assuming a mass–luminosity relation  $M_\odot \sim L_\odot$ .

Cluster	$\sigma$ (km s <sup>-1</sup> )	$r_0$ (pc)	$\rho_0$ ( $M_\odot$ pc <sup>-3</sup> )	$c_{\text{GC}}$
NGC 7078 (M 15)	10.8	0.42	$1.12 \times 10^5$	2.29
Liller 1	5.05	0.15	$1.90 \times 10^5$	2.3
NGC 5139 ( $\omega$ Cen)	10.2	3.58	$1.41 \times 10^3$	1.31
NGC 6626 (M 28)	7.8	0.38	$7.24 \times 10^4$	1.67

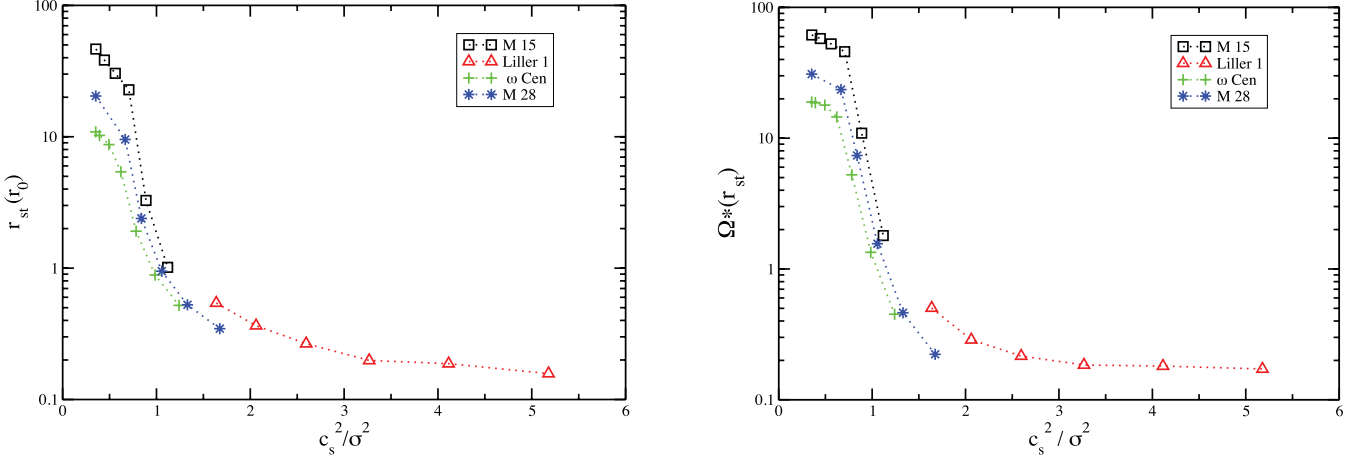


**Figure 1.** Stagnation radius and accretion rate versus gas temperature for different clusters (squares for M 15, triangles for Liller 1, plus signs for  $\omega$  Cen and stars for M 28). The adimensional black hole mass  $\Omega_{\text{BH}}$  is  $\sim 0.007$  in all cases. A decreasing profile arises and the curves are placed in the graph ordered with increasing central cluster potential (from bottom to top).

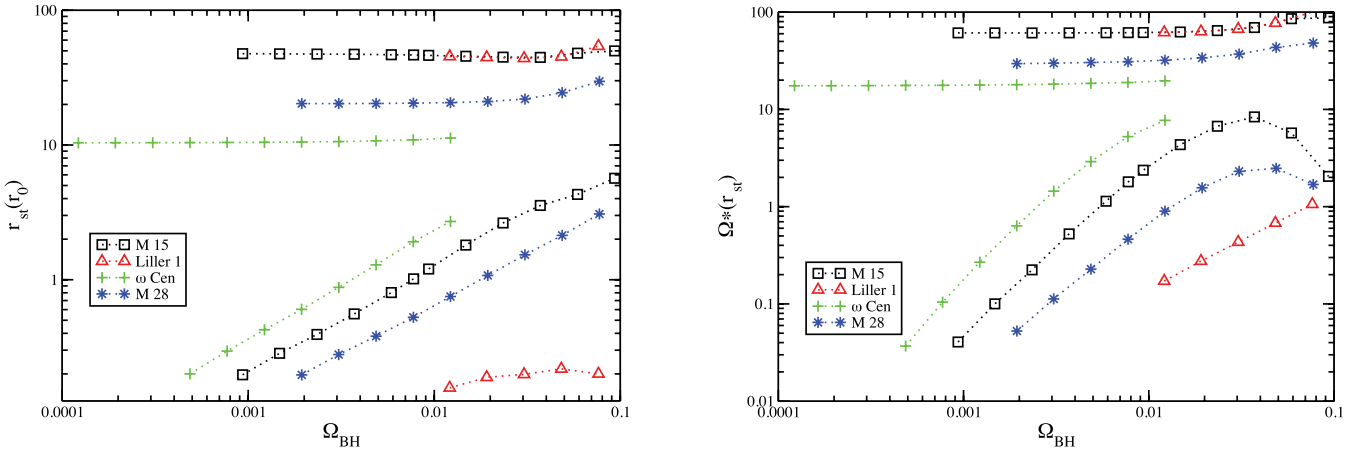


**Figure 2.** Stagnation radius and accretion rate versus black hole mass for different clusters (squares for M 15, triangles for Liller 1, plus signs for  $\omega$  Cen and stars for M 28). The adimensional temperature  $c_s^2/\sigma^2$  is  $\sim 0.34$  for all the clusters in the HAR regime (upper set of curves). For those in a LAR regime (lower set of curves) the adimensional temperature is around 1, except for Liller 1, for which it is  $\sim 3$ . The curves are placed in the graph ordered with increasing central cluster potential (from bottom to top). It can be seen that the dependence of the accretion rate on the black hole mass can be neglected compared to the temperature dependence.

masses the assumption of the IMBH at rest at the centre of the cluster would not hold.

In Figs 1 and 2 we show the stagnation radius  $\xi_{\text{st}}$  and the (non-dimensional) accretion rate  $\Omega(\xi_{\text{st}})$  as a function of the free parameters  $c_s/\sigma$  and  $\Omega_{\text{BH}}$ , respectively, with the other parameter kept fixed. It is worth pointing out that the true accretion rate  $\dot{M}$  can be recovered via  $\dot{M} = \alpha \Omega(\xi_{\text{st}}) \rho_0 r_0^3$ , with a suitable value for  $\alpha$  (see Section 4 for a discussion). It can be seen from the left-hand panel of Fig. 1 that the stagnation radius decreases with the ratio  $c_s/\sigma$ . This can be easily understood in terms of the energetics of the gas: for higher temperatures the gas has more energy and can escape from inner regions of the cluster, where the gravitational well is deeper, hence moving the stagnation radius inwards. This results in a lower accretion rate (right-hand panel). It is interesting to note that the stagnation radius curve steepens at  $r_{\text{st}} \sim r_0$ , where  $c_s/\sigma \sim 1$ . The rapid increase of the stellar mass of the cluster at this radius results then in an abrupt change in the accretion rate. This abrupt change suggests the existence of two accretion regimes: at high temperatures ( $c_s/\sigma > 1$ ), the stagnation radius is located in the central region of the cluster ( $r_{\text{st}} \lesssim r_0$ ) resulting in a low accretion rate

(LAR), while at low temperatures ( $c_s/\sigma < 1$ ) the stagnation radius is far from the centre ( $r_{\text{st}} \gg r_0$ ) resulting in a high accretion rate (HAR). Note that the accretion rate differs by almost three orders of magnitude between the LAR and the HAR. Fig. 1 shows another characteristic differentiating the HAR from the LAR. In the former, the stagnation radius and the accretion rate increase with the cluster concentration  $c_{\text{GC}}$ .

Fig. 2 shows the dependence of the stagnation radius and accretion rate on the non-dimensional IMBH mass, at a fixed non-dimensional temperature. Two temperatures were explored, one resulting in the LAR and the other in the HAR. Both the stagnation radius and the accretion rate are almost independent of  $\Omega_{\text{BH}}$  in the HAR regime. This happens because far from the centre the IMBH has no influence on the stellar distribution, and the stellar mass increases very slowly. On the other hand, in the LAR regime there is a strong dependence on the IMBH mass, because the stagnation radius is near the sphere of influence where the stellar distribution becomes dominated by the IMBH. Note that in this regime, the accretion rate varies also with the cluster concentration, decreasing as the latter increases. In Fig. 3 we show the ratio between the

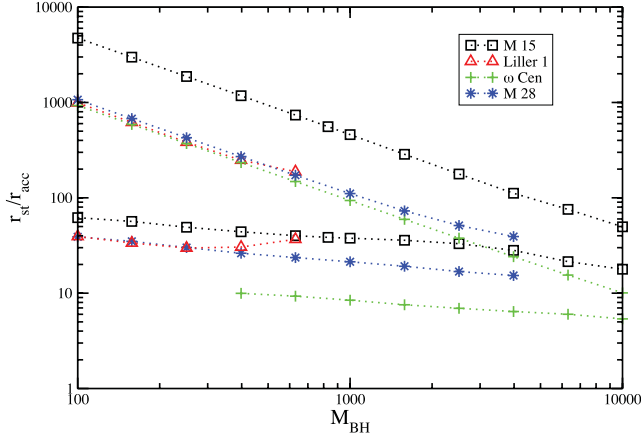


**Figure 3.** Ratio between the stagnation radius and the accretion radius of black hole. In the LAR regime the stagnation radius behaves like the accretion radius.

stagnation radius and the accretion radius defined as  $r_{\text{acc}} = GM_{\text{BH}}/c_s^2$ . It can be seen that in the HAR regime, since the stagnation radius remains independent of the black hole mass, the ratio  $r_{\text{st}}/r_{\text{acc}}$  decreases with increasing  $M_{\text{BH}}$ . In the LAR regime, this ratio remains almost constant implying that  $\dot{M}$  scales as  $\sim M_{\text{BH}}^2$  like in the traditional Bondi–Hoyle model. However, the ratio is one to two orders of magnitude greater than unity, and hence the accretion rate at a fixed IMBH mass is much higher in our models than in the Bondi–Hoyle case.

### 3.2 Milky Way globular clusters

In the previous section, we have shown that in some cases there is a dependence of the accretion rate on the cluster properties. Here we explore this dependence by applying the scheme detailed in Section 2 to the Milky Way GCs with well-determined parameters (listed in the catalogue of Harris 1996), to construct flow models for different temperatures and IMBH masses. It is worth pointing out that the results from Section 2 extend to all the clusters in the catalogue and the same reasoning can be applied to them. For

each model, the accretion rate was computed using the same value of  $\alpha$  as in the previous section. In some cases, the models were discarded because the IMBH mass was not much lower than the cluster mass, while in others no stagnation radius was found for the hottest temperatures (the ICM escapes completely as a wind). We searched for correlations between the accretion rate and the properties of the cluster, defined by their scaling parameters and masses. We found no trend for the accretion rate  $\dot{M}$  with  $r_0$  or  $\rho_0$ , but a clear correlation with the cluster mass  $M_{\text{GC}}$  and velocity dispersion parameter  $\sigma$ .

We show in Fig. 4 the dependence between  $\dot{M}$  and  $\sigma$  for a conservative value of the IMBH mass,  $M_{\text{BH}} = 1000 M_{\odot}$  and three different temperatures  $T = 5000, 10\,000, 12\,600$  K (left-hand panel), and for a fixed gas temperature ( $T = 5000$  K) and different IMBH masses  $M_{\text{BH}} = 1000, 4000, 10\,000 M_{\odot}$  (right-hand panel). The clear trend observed in the left-hand panel is understood in terms of the results of the previous section. For a fixed value of  $T$ , an increase in  $\sigma$  implies a decrease in  $c_s/\sigma$ , changing the flow from the LAR upwards to the HAR in the curves defined in Fig. 1. This explains why the GCs with higher  $\sigma$  are more likely to be found in an HAR regime. The change in the location of the curve as the temperature increases is also consistent with this interpretation. The dispersion of this correlation is in part due to the different concentrations of the GCs, and in part to the fact that  $\dot{M}$  scales as  $\rho_0 r_0^3$ , which is different for each cluster. The right-hand panel of Fig. 4 shows that the effect of the IMBH mass for a fixed temperature is small.

A trend of increasing accretion rate with the cluster mass can also be seen in Fig. 5 for HARs. This is explained by the fact that these clusters are accreting in the HAR regime, for which the stagnation radius is well outside the cluster core and hence encloses almost the whole cluster stellar mass. As  $\dot{M}$  is proportional to the stellar mass inside  $r_{\text{st}}$ , the correlation with  $M_{\text{GC}}$  arises. In other words, most of the mass ejected by the stars in the cluster is accreted by the IMBH. As the cluster is more massive, more mass is available to be accreted, which explains the clear trend with  $M_{\text{GC}}$  in the HAR regime. Note that this trend is independent of the temperature and IMBH mass (as far as the accretion proceeds in the HAR regime), and it is very tight because both  $\dot{M}$  and  $M_{\text{GC}}$  scale with the same combination of parameters of the cluster ( $\rho_0 r_0^3$ ), reducing the dispersion due to the scaling from non-dimensional to physical variables. For clusters

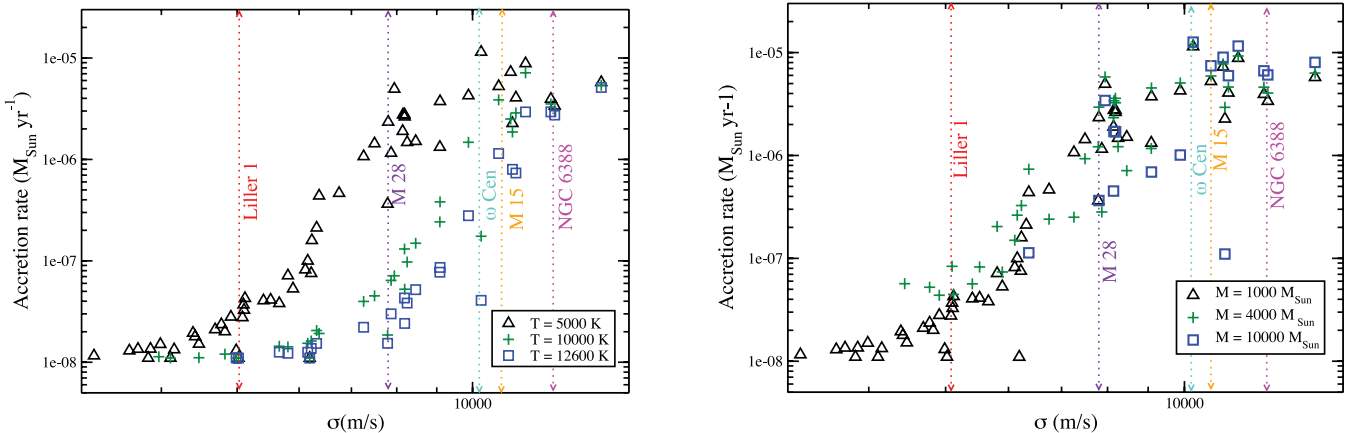


**Figure 4.** Accretion rate versus GC velocity dispersion ( $\sigma$ ) for three different temperatures (left-hand panel): 5000 K (triangles), 10 000 K (plus signs) and 12 300 K (squares). Accretion rate versus GC velocity dispersion for three different black hole masses (right-hand panel):  $1000 M_{\odot}$  (triangles),  $4000 M_{\odot}$  (plus signs) and  $10\,000 M_{\odot}$  (squares). There is a nearly constant value of  $\dot{M}$  for those clusters with low  $\sigma$ . The clusters located in the right end of the curve are those clusters accreting at an HAR regime. The dotted lines indicate the  $\sigma$  values corresponding to the clusters from Section 2 and the particular case of NGC 6388 discussed in Section 4.

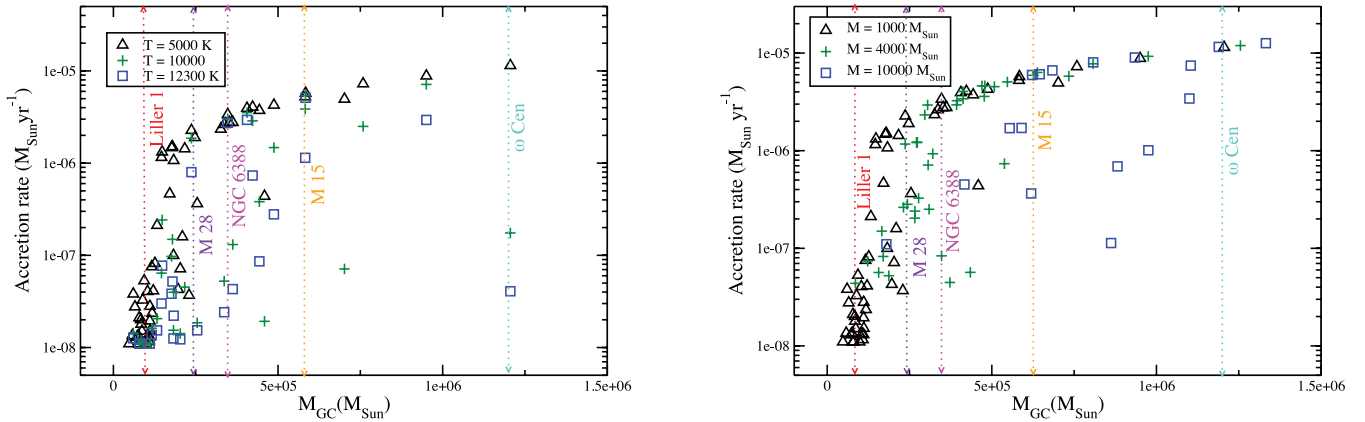


**Figure 5.** Accretion rate versus GC mass for three different temperatures (left-hand panel): 5000 K (triangles), 10 000 K (plus signs) and 12 300 K (squares). Accretion rate versus GC mass for three different black hole masses (right panel):  $1000 M_{\odot}$  (triangles),  $4000 M_{\odot}$  (plus signs) and  $10\,000 M_{\odot}$  (squares). A soft trend can be observed, although there is a wide spread of the data. The dotted lines indicate the  $M_{GC}$  values corresponding to the clusters from Section 2 and the particular case of NGC 6388 discussed in Section 4.

in the LAR regime there is no clear trend, as the small stagnation radius decouples the accretion rate from the cluster mass. According to the results of this section, the clusters with large values of  $\sigma$  and high  $M_{GC}$  are most likely to be in an HAR regime, and are therefore the best candidates to perform detections of the accretion on to an IMBH.

### 3.3 Differences with the Bondi–Hoyle model

The model presented in this paper differs from that of Bondi & Hoyle (1944) in some very fundamental aspects. Our model takes into account the gravitational potential of the cluster, which differs from cluster to cluster, and also includes the constant injection of gas into the ICM by the red giants of the cluster; hence, the black hole is no longer accreting from a static and infinite medium. These two features of our model produce a very important consequence, which is its main difference from the Bondi–Hoyle result: the accretion rate not only depends on the black hole mass and gas temperature (or the sound speed), but also on the cluster properties. Fig. 6 shows the comparison between our model (for different clusters; all of them at  $T = 10000$  K), the Bondi–Hoyle accretion rate and the Eddington rate  $\dot{M}_{Edd} = L_{Edd}/c^2$ , where  $c$  is the speed of light and  $L_{Edd} =$

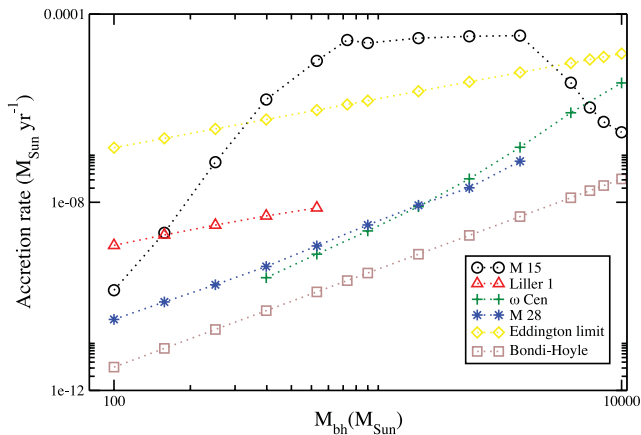


**Figure 6.** Comparison between our accretion rate and Bondi–Hoyle accretion rate. We also show the Eddington accretion rate for a reference.

$1.26 \times 10^{38} (M_{BH}/M_{\odot}) \text{ erg s}^{-1}$  is the Eddington luminosity of the IMBH. The Bondi–Hoyle accretion rate was calculated as  $\dot{M}_{BH} = 4\pi G^2 M_{BH}^2 \rho_a c_s^{-3}$ , where  $\rho_a$  is the ambient gas density. We used the value  $\rho_a = 0.2 \text{ cm}^{-3}$  (Freire et al. 2001), which is the same value used by other authors (e.g. Maccarone 2004) to compute IMBH X-ray luminosities. To make the results of our models comparable to those obtained with the Bondi–Hoyle scenario, for each of our models we have chosen the fractional mass-loss rate of the stars  $\alpha$  so that the density at the stagnation radius matches  $\rho_a$ . This choice is justified because it makes both models to have the same density at the point where the fluid is at rest. The values of  $\alpha$  obtained are in the range  $10^{-14}$ – $10^{-11} \text{ yr}^{-1}$ , in rough agreement with (but somewhat lower than) the few observational estimations of this parameter (Scott & Rose 1975; Priestley et al. 2011).

It can be seen from Fig. 6 that the accretion rate in the HAR regime (such as that of NGC 7078 in this plot) no longer scales as  $M_{BH}^2$ , and that it is cluster dependent. However, in the LAR regime the behaviour is similar to that of Bondi–Hoyle models, although the absolute value of  $\dot{M}$  is one order of magnitude higher. Another interesting result seen in this figure is that in the HAR regime, IMBHs reach accretion rates as high as the Eddington values (assuming a 100 per cent efficient conversion of gravitational energy into radiation). This result is due to the development of a cluster-wide flow in the HAR regime, which carries matter from the outer regions on to the IMBH to produce an HAR. It cannot be reproduced by the Bondi–Hoyle model unless a very high density or very low temperature is assumed. This result is important for the explanation of the emission of ULXs, as will be discussed in the next section. It is worth pointing out that these flows with super-Eddington accretion rates do not imply super-Eddington luminosities as the radiation efficiency is usually much lower than 1. Hence, these flows can still proceed without being stopped by radiation pressure.

## 4 DISCUSSION

In this work, we developed a simple model for the accretion of the ICM of a GC on to an IMBH at its centre. Bearing in mind that the detection of ongoing accretion would be a strong piece of evidence for the existence of these elusive black holes, our aim was to refine the predictions of the expected accretion rate, improving on the

(usually assumed) classical Bondi–Hoyle accretion. In particular, we explored the consequences of including the effect of the gravitational field of the cluster and the fluid sources on the flow. Our models aim at assessing the influence of the cluster as a whole on the accretion flow, which was suggested to be important in the case of cosmological fluids such as dark matter by Pepe et al. (2012).

We made several assumptions in our model, namely that the flow is stationary, spherically symmetric and isothermal. While the first two can be regarded as working hypotheses made to simplify the computations, the latter can be a good approximation for the whole cluster (Scott & Rose 1975). However, it may break down very near the black hole, where the transformation of gravitational into thermal energy is higher and may heat the gas in time-scales shorter than the cooling one. Although our model could not describe the dynamics of the flow in these spatial scales, it is still useful to assess the existence of cluster-wide flows, whose dynamics is governed by phenomena occurring at much larger spatial scales, and estimates the order of magnitude of the accretion rate produced by these flows. To analyse the details of the flow very near the black hole, we are currently developing more complex models which include several heating and cooling mechanisms.

Our main results are the following. First, large-scale flows can form in GCs with IMBHs, due to the influence of the gravitational field of the cluster and the mass-loss of the cluster stars. These flows show a stagnation radius at which the velocity is null. Outside this radius, the ICM escapes from the cluster as a wind, as the energy of the flow allows it to overcome the cluster potential well. Inside the stagnation radius the ICM is retained by the potential well, and an accretion flow on to the IMBH develops. As our models are stationary, the accretion rate on to the IMBH is determined by the stagnation radius and the mass-loss rate of the stars.

The accretion rate on to the IMBH in a given cluster depends mainly on the ratio of the sound speed in the ICM to the stellar velocity dispersion parameter. This is a consequence of the energetics of the flow, and the same effect was observed by Pepe et al. (2012) for dark matter. The sound speed (related to the temperature of the flow) measures the internal energy of the ICM, while the stellar velocity dispersion parameter indicates the strength of the cluster gravitational field. As the ratio of these two magnitudes increases, the ratio of the internal to gravitational energy of the flow increases as well, making easier for the ICM to escape from the cluster. Therefore, the stagnation radius decreases, the wind becomes stronger and the accretion flow weaker, diminishing the accretion rate.

The stellar-mass distribution of GCs has also important effects on the flow. These clusters show a large concentration of their mass within a few core radii of their centres, while the potential well of the cluster extends to far beyond (typically to tidal radii one or two orders of magnitude larger than the core radius). This translates into a steep increase of the accretion rate when the temperature is low enough for the stagnation radius to reach the core radius, as most of the cluster stellar mass (and hence most of the stellar mass-loss) is enclosed within the latter. This steep increase separates two accretion regimes with different properties, one with an HAR at low temperatures and the other with an LAR at higher temperatures.

In the HAR regime, for a fixed temperature the accretion rate is high, proportional to the cluster mass, and almost independent of the IMBH mass, as far as the IMBH is not massive enough to severely change the whole cluster mass distribution (however, if this were the case, strong signatures of the presence of the black hole should be found in the stellar distribution and dynamics). The dependence

of the accretion rate on the cluster mass instead on the IMBH mass is due to the fact that in the HAR regime, the stagnation radius is in the outer region of the GC, and the IMBH accretes a major fraction of the mass lost by the stars, which is proportional to the cluster mass. Note the difference with the classical Bondi–Hoyle model, in which the accretion rate scales as the square of the black hole mass.

The LAR regime is qualitatively different, showing accretion rates several orders of magnitude lower, which depend strongly on the IMBH mass. The accretion rates in the LAR regime are still one order of magnitude greater than the Bondi–Hoyle prediction for similar boundary conditions, and depend on the IMBH mass because the stagnation radius is near or inside the IMBH sphere of influence. This dependence varies from cluster to cluster due to the different stellar-mass profiles of the clusters, but on average it mimics the  $M_{\text{BH}}^2$  dependence of the Bondi–Hoyle model.

Another strong assumption of our models is that the IMBH is at rest at the centre of the cluster. This approximation holds because the mass of the IMBH is far greater than the mass of the stars in the cluster. Assuming that the stars in the cluster have a mean mass of  $\sim 0.5 M_{\odot}$  and a mean velocity of the order of  $\sigma$ , energy equipartition implies that the IMBH would have a velocity of the order of  $\sigma/2\sqrt{M_{\text{BH}}/M_{\odot}}$ . At these velocities, and taking into account that  $c_s/\sigma \sim 1$  in our models, the typical correction to the accretion rate due to the motion of the IMBH with respect to the flow (Hoyle & Lyttleton 1939) would be less than 1 per cent. Hence, neglecting this effect is justified for these models.

The application of our model to the Milky Way GCs has shown that the higher accretion rates are predicted for those clusters with the largest values of the velocity dispersion parameter  $\sigma$ . However, the higher the temperature of the gas, the higher the minimum value of  $\sigma$  for GCs accreting at high rates. This result suggests that the signatures of the accretion on to IMBHs must be searched for in GCs with high velocity dispersion parameters and low gas temperatures. All the clusters that were observationally proven so far for the existence of IMBHs satisfy the first criterion. The satisfaction of the criterion on gas temperature is difficult to assess, as measurements of the ICM thermodynamical state are still rare (e.g. Freire et al. 2001). As pointed out by Scott & Rose (1975), the temperature of the flow depends mainly on that of the radiation field to which it is exposed; hence, a proxy for the former would be the number of UV sources within the cluster, such as blue horizontal branch stars or blue stragglers. These sources would heat the gas, preventing the accretion flow to develop out to large scales, and hence decreasing the accretion rate. Interestingly, Miocchi (2007) argues that extreme horizontal branch stars with strong UV fluxes might be the result of the stripping of normal stars passing near the IMBH. If this is indeed the case, the presence of the IMBH would help in heating the flow, decreasing the accretion rate.

From the results of our model we can estimate the X-ray luminosity  $L_X$  due to the accretion process on to the IMBH. However, in our model the luminosity depends linearly on two poorly constrained parameters, the fractional mass-loss rate of the stars  $\alpha$  and the accretion efficiency of the flow,  $\epsilon = L_X/\dot{M}c^2$ . If we adopt the standard values,  $\epsilon = 0.1$  for accreting stellar-mass black holes and  $\alpha = 10^{-11} \text{ yr}^{-1}$ , the luminosities produced by the accretion flows of our models would be in the range  $10^{37} - 10^{41} \text{ erg s}^{-1}$ . The high end of this range is in good agreement with the luminosities of ULXs. If, as claimed in a few cases, there are ULXs positionally coincident with extragalactic GCs (Angelini, Loewenstein & Mushotzky 2001; Maccarone et al. 2011, and references therein), our models suggest that these systems may contain IMBHs accreting in the HAR regime at the centres of GCs, with standard accretion efficiencies.

In the case of NGC 6388 our models predict (based on the estimation of the accretion rate and assuming the efficiencies discussed above) X-ray luminosities in the range  $10^{38} - 10^{40}$  erg s $^{-1}$ , at least five orders of magnitude higher than the observed value of  $L_{X,NGC\ 6388} = 2.7 \times 10^{33}$  erg s $^{-1}$ . However, the prediction can be reconciled with observations if either  $\alpha$  or  $\epsilon$  is lower. Nucita et al. (2008) reached the same conclusion about the efficiency. It is worth mentioning that different theoretical models have been developed for accretion flows with very low efficiencies, such as advection-dominated accretion flows (ADAFs; Narayan & Yi 1994), jet-dominated accretion flows (Fender, Gallo & Jonker 2003) and low-radiative efficiency accretion flows (Quataert 2001). For example, in the case of ADAFs the efficiency scales as  $\epsilon = \dot{M}/\dot{M}_{Edd}$  for  $\dot{M} < 0.1\dot{M}_{Edd}$ , giving in our case estimations of the luminosity two to three orders of magnitude lower, approaching the observational limits. On the other hand, the value of  $\alpha$  is highly uncertain, relying on theoretical models and with a few observational constraints (Scott & Rose 1975; McDonald et al. 2011; Priestley et al. 2011). Given that the low-luminosity limits of our predicted range correspond to low IMBH masses, we conclude that such an IMBH accreting in the LAR is a possible explanation for the central engine of the central X-ray source in NGC 6388. The case of G1 is slightly different, as this cluster is so massive that the luminosity in the HAR is  $L_X \sim 10^{42}$  erg s $^{-1}$ , and the development of an LAR requires temperatures of several times 10 000 K. As the observed luminosity is only  $L_X = 2 \times 10^{36}$  erg s $^{-1}$ , it is difficult to reconcile it with the predictions, unless the G1 ICM is strongly heated, the accretion efficiency is extremely low, or its stars lose mass at very low rates. The Galactic GCs with undetected central X-ray sources, with measured upper limits of  $10^{31} - 10^{32}$  erg s $^{-1}$  for their X-ray luminosities, are in the same case.

The models presented in this work explore the consequences of taking into account the gravitational field of the GC and the mass-loss by stars in the computation of the accretion rate on to an IMBH in the centre of a GC. Although they are very simple, they allow us to get some insight into the development of cluster-wide flows that may feed these compact objects. Many improvements can be made on the models, such as relaxing the isothermal hypothesis to include the detailed physics of gas heating and cooling, or including the radiation pressure on the flow due to the X-ray emission of the flow itself. At present we are working on these tasks, which require a more complex numerical approach to the problem. We expect that with an improved physical model that gives more precise predictions on the accretion rates and luminosities, and with detailed stellar evolution models that predict stellar mass-loss rates, deeper X-ray measurements and ICM observations, we would be able to determine the existence or not of these elusive compact objects and put limits on their masses.

## ACKNOWLEDGMENTS

We thank the anonymous referee for her/his comments and suggestions, which really helped to improve our manuscript. We acknowledge financial support by Argentine ANPCyT through grant PICT-2007-0848.

## REFERENCES

Angelini L., Loewenstein M., Mushotzky R. F., 2001, *ApJ*, 557, 35  
 Baumgardt H., Makino J., Hut P., McMillan S., Portegies Zwart S., 2003, *ApJ*, 589, 25

Bondi H., Hoyle F., 1944, *MNRAS*, 104, 273  
 Dupree A. K., Hartmann L., Smith G. H., Rodgers A. W., Roberts W. H., Zucker D. B., 1994, *ApJ*, 421, 542  
 Fender R. P., Gallo E., Jonker P. G., 2003, *MNRAS*, 343, 99  
 Feng H., Soria R., 2011, *New Astron. Rev.*, 55, 166  
 Frank J., King A., Raine D., 2002, 'Accretion Power in Astrophysics. Cambridge Univ. Press, Cambridge  
 Freire P. C., Kramer M., Lyne A. G., 2001, *ApJ*, 557, 105  
 Fryer C., Kalogera V., 2001, *AJ*, 554, 548  
 Fusi Pecci F., Renzini A., 1975, *A&A*, 39, 413  
 Gallo E., Fender R. P., Pooley G. G., 2003, *MNRAS*, 344, 60  
 Gebhardt K., Rich R. M., Ho L. C., 2002, *ApJ*, 578, 41  
 Harris W. E., 1996, *AJ*, 112, 1487  
 Hoyle F., Lyttleton R. A., 1939, *Proc. Cambridge Philosophical Society*, Vol. 35, p. 405  
 King I. R., 1966, *AJ*, 71, 276  
 King A. R., Davies M. B., Ward M. J., Fabbiano G., Elvis M., 2001, *ApJ*, 552, L109  
 Knapp G. R., Gunn J. E., Bowers P. F., Vasquez Poritz Justin F., 1996, *ApJ*, 462, 231  
 Kong A. K. H., Heinke C. O., di Stefano R., Cohn H. N., Lugger P. M., Barmby P., Lewin W. H. G., Primini F. A., 2010, 407, 84  
 K rding E., Falcke H., Markoff S., 2002, *A&A*, 382, L13  
 Maccarone T. J., 2004, *MNRAS*, 351, 1049  
 Maccarone T. J., Kundu A., Zepf S. E., Rhode K. L., 2011, *MNRAS*, 410, 1655  
 Magorrian J. et al., 1998, *AJ*, 115, 285  
 Mauas P. J. D., Cacciari C., Pasquini L., 2006, *A&A*, 454, 609  
 McDonald I., Boyer M. L., van Loon J. Th., Zijlstra A. A., 2011, *ApJ*, 730, 71  
 McLaughlin D. E., Anderson J., Meylan G., Gebhardt K., Pryor C., Minniti D., Phinney S., 2006, *ApJS*, 166, 249  
 Miller M. C., Hamilton D. P., 2002, *MNRAS*, 330, 232  
 Miller-Jones J. C. A. et al., 2012, 755, 6  
 Miocchi P., 2007, *MNRAS*, 381, 103  
 Narayan R., Yi I., 1994, *ApJ*, 428, L13  
 Noyola E., Gebhardt K., 2006, *AJ*, 132, 447  
 Noyola E., Gebhardt K., Kissler-Patig M., L tzgendorf N., Jalali B., de Zeew P. T., Baumgardt H., 2010, *ApJ*, 719, 60  
 Nucita A. A., De Paolis F., Ingrassio G., Carpano S., Guainazzi M., 2008, *A&A*, 478, 763  
 Pepe C., Pellizza L. J., Romero G. E., 2012, *MNRAS*, 420, 3298  
 Portegies Zwart S. F., Baumgardt H., Makino J., McMillan S. L., Hut P., 2004, *Nat*, 428, 724  
 Priestley W., Ruffert M., Salaris M., 2011, *MNRAS*, 411, 1935  
 Quataert E., 2001, in Peterson B. M., Pogge R. W., Polidan R. S., eds, *ASP Conf. Ser. Vol. 224, Probing the Physics of Active Galactic Nuclei*. Astron. Soc. Pac., San Francisco, p. 71  
 Roberts M. S., 1988, in Grindlay J. E., ed., *Proc. IAU Symp. 126, The Harlow Shapley Symposium on Globular Clusters Systems in Galaxies*. Kluwer, Dordrecht, p. 441  
 Scott E. H., Rose W. K., 1975, *ApJ*, 197, 147  
 Ulvestad J. S., Greene J. E., Ho L. C., 2007, *ApJ*, 661, 151  
 van den Bosch R., de Zeeuw T., Gebhardt K., Noyola E., van de Ven G., 2006, *ApJ*, 641, 852  
 van der Marel R., Anderson J., 2010, *ApJ*, 710, 1063